ARTICLE

Elasto-plastic Analysis of High-strength Concrete Shear Wall with Boundary Columns Using Fiber Model

Xiaolong Tong[1*]   Yangjing Ou[1]   Sixi Xiao[1]   Jianliang Wu[1]   Fumin Chen[2]

1. College of Civil Engineering, Hunan Institute of Science and Technology, Yueyang, 414000, China
2. Nanhu College, Hunan Institute of Science and Technology, Yueyang, 414000, China

ABSTRACT

In this study, an experimental study and numerical calculations using fiber model were conducted for four high-strength concrete shear walls with boundary columns under low cyclic load. The boundary column and shear wall were divided into fiber elements, and PERFORM-3D finite element analysis software was used to carry out push-over analysis on the test specimens. The results show that the finite element analysis results were in good agreement with the experimental results. The proposed analysis method could perform elasto-plastic analysis on the high-strength concrete shear wall with boundary columns without distinguishing the categories of frame column and shear wall. The seismic performance of high-strength concrete shear wall with boundary columns was analyzed using the following parameters: axis compression ratio, height to width ratio, ratio of vertical reinforcement, and ratio of longitudinal reinforcement in the boundary column. The results show that the increase in the axial compression ratio causes the bearing capacity of the shear wall to increase at first and then to decrease and causes the ductility to decrease. The increase in the height to width ratio causes the bearing capacity of the shear wall to decrease and its ductility to increase. The ratio of vertical reinforcement was found to have little effect on the bearing capacity and ductility. The increase in the ratio of longitudinal reinforcement in boundary column resulted in a significant increase in the bearing capacity and caused the ductility to decrease at first and then to slowly increase.

1. Introduction

Use italic for emphasizing a word or phrase. Do not use boldface typing or capital letters except for section headings (cf. remarks on section headings, below). As the name implies, high-strength concrete exhibits very high-strength. In addition it has several other advantages, such as high elastic modulus, durability, good impermeability, and leak resistance. High-strength reinforced concrete used in high-rise and super high-rise buildings can reduce the size of the shear wall section and the structure weight. However, high-strength concrete is very brittle and causes a poor deformation ability of the shear wall. Therefore, improving the seismic behavior of high-strength concrete shear walls is very important. Studies showed that the seismic performance of high-strength concrete shear walls could be effectively improved by setting boundary columns at both ends of the wall [1]. This approach was

---

*Corresponding Author:
Xiaolong Tong,
College of Civil Engineering, Hunan Institute of Science and Technology, Yueyang, 414000, China;
Email: txlpaper@outlook.com

found also to improve the wall's ductility index to meet the design requirements. The common analysis methods of shear walls with boundary columns are to equate the column with the wall or to separate the wall and column. One disadvantage of the later is that the deformation co-ordination of wall and column elements in the adjacent boundary cannot be guaranteed and the bearing capacity of members is underestimated [2]. In this study, PER-FORM-3D finite element software and fiber model were used to perform nonlinear numerical simulation of high-strength concrete shear wall with boundary columns. This is a nonlinear analysis method for high-strength concrete shear walls with side columns, which can be used in engi-neering applications, because it can meet the engineering requirements with sufficient accuracy.

Establishment of Numerical Model

PERFORM-3D software, formerly known as the Drain-3D program, was developed by Professor Powell from the University of California, Berkeley [3]. It mainly uses fiber unit model to perform seismic elasto-plastic analysis of complex and super high-rise buildings. PERFORM-3D adopts fiber wall unit to be used with shear walls. Axi-al-bending characteristics of shear walls are represented by concrete fiber and reinforcement fiber sections. Shear characteristics are represented by elastic or elasto-plastic shear materials. In PERFORM-3D, the shear wall unit based on the fiber model is constructed according to the multi-vertical bar element model (MVLEM) theory [4] (Fig.1). The fiber wall element satisfies the assumption of flat section, and hence the upper and lower parts of the element are always rigid rods that are used to maintain the plane. Vertical spring $k_{v1}, k_{v2}... k_{vn}$ simulates the bending effect of the entire wall section, and the horizontal spring k_s simulates the shear dislocation deformation at the top and bottom.
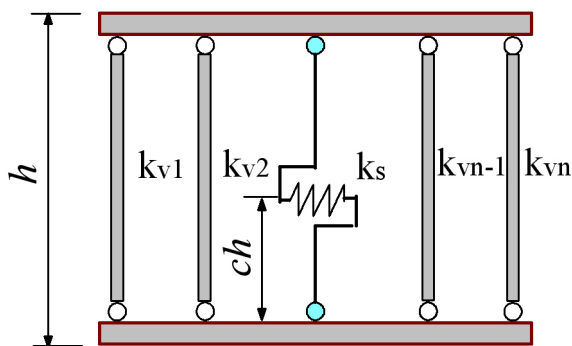

Figure 1. Schematic diagram of the MVLEM unit

PERFORM-3D shear wall fiber model separately defines reinforcement and concrete fiber units and then assembles them. The end restraint area can be simulated using con-fined concrete fiber. The shear wall with boundary column analyzed in this study divided both boundary column and shear wall into fiber elements (Fig.2) without distinguishing between the column and the wall components. In the shear wall simulation, the vertical grid division was carried out for the height of the shear wall. The length of the vertical elements is determined based on the FEMA356 recommen-dation [5], taking half of the wall length. The axial force was applied to the joint at the top of the wall.
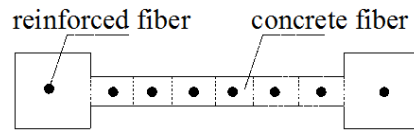

Figure 2. Fiber section division

2. Material Constitutive Model

2.1 Concrete

The boundary column concrete was simulated using the Mander constrained concrete constitutive model [6]. The concrete in the web part was considered to be un-constrained and was modeled according to the stress-strain curve provided in appendix C of *Code for design of concrete structures* [7]. However, tensile strength was not considered in both restrained and unrestrained concretes.

PERFORM-3D software restricted that the concrete con-stitutive curve can only be composed of multiple broken lines, as shown in Fig.3. In Fig.3, Y is the yield point, U is the peak point, UL is the transient horizontal segment, L is the beginning of the stress decline, R is the residual stress value, and X is the material maximum deformation point. In this study, the constitutive relationship of concrete was fitted assuming that the enclosed area under the broken line segment and the enclosed area under the Code curve were equal [8]. In addition, initial stiffness of the broken line is assumed to be the value of the elastic modulus.
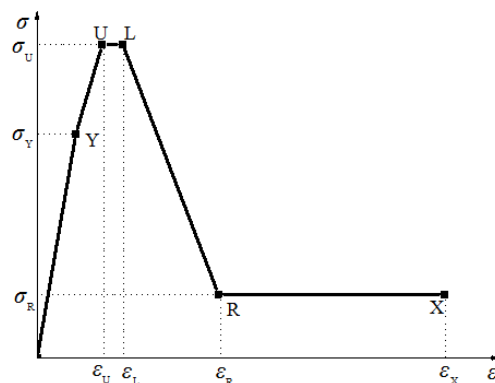

Figure 3. Concrete multi-line constitutive relationship under axial compression

2.2 Rebar

The rebars were simulated according to the three-fold constitutive model (Fig.4), where f_Y is the yield strength, f_U is the ultimate strength, and the stiffness reinforcement coefficient is 0.01.
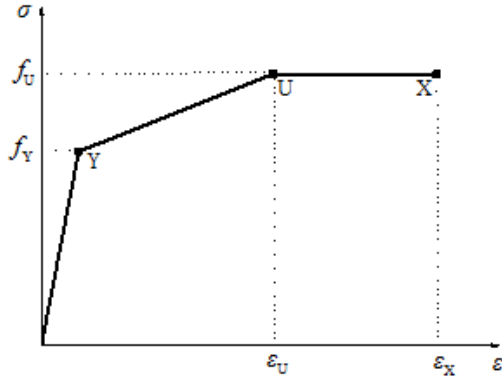

**Figure 4.** Reinforcement constitutive relationship

## 3. Calculation Results and Parameter Analysis

3.1 The Experiment

Following reference [1], four high-strength concrete shear walls with boundary columns were selected for numerical simulation. The height of the specimen section was 1000 mm, while the dimensions of the boundary column and wall web sections were 200 mm × 200 mm and 600 mm × 100 mm, respectively, (Fig.5). C80 concrete was used as the high-strength concrete. Table 1 shows the basic parameters of the specimen as well as the strength of reinforced concrete. The diameter of the stirrups in all specimens was 5 mm. The spacing between the stirrups of DHPCW-01 and DHPCW-03 was 30 mm and between those of DHPCW-02 and DHPCW-04 was 40 mm. The ultimate tensile strength of stirrup was 737.5 MPa. Table 2 shows the mechanical properties of the reinforcement bars obtained from the test.
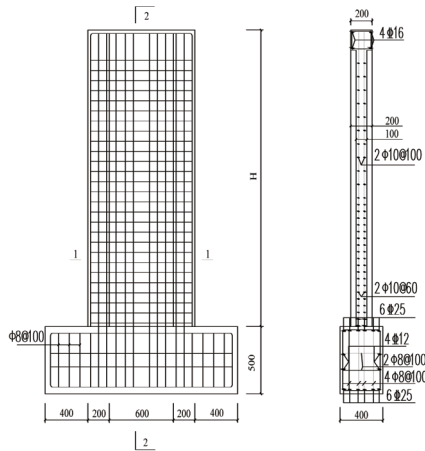
(a) Elevation view   (b) Elevation view 2-2
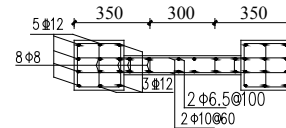
(c) Elevation view 2-2 of DHPCW-01and 03
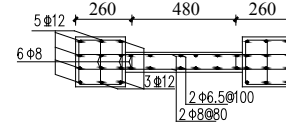
(d) Elevation view 2-2 of DHPCW-02 and 04

Figure 5. Geometry and reinforcement of specimens (mm)

Table 1. Parameters of the specimen

Specimen number	H/mm	Height to width ratio	Cube compressive strength /Mpa	Axial compression ratio
DHPCW-01	2200	2.1	94.22	0.28
DHPCW-02	2200	2.1	96.89	0.21
DHPCW-03	1600	1.5	99.56	0.21
DHPCW-04	1600	1.5	89.33	0.21

Table 2. Mechanical properties of rebars

Reinforcement type	f_Y (N/mm²)	f_U (N/mm²)
$\Phi25$	485.1	654.3
$\Phi16$	452.9	614.6
$\Phi12$	460.0	667.9
$\Phi10$	494.0	575.2
$\Phi8$	474.2	579.0
$\Phi6.5$	419.3	550.3

Horizontal loads were applied by reciprocating actuators and the horizontal loading point was located in the center of the loading beam at the top of the wall. Figure 6 shows the loading device, in which the vertical load was provided by vertical hydraulic jack. A horizontal load was applied by an electro-hydraulic servo actuator. The cyclic horizontal load is controlled by a mixture of force and drift. Cracks occurred at the bottom of all boundary columns of all specimens. As the load increased, the cracks in the boundary columns extended to the wallboard and developed to the upper part of the specimens. Finally, the concrete at the bottom of the boundary columns and webs was crushed, and the longitudinal reinforcement was folded and exposed. Bending failure occurred in specimens DHPCW-01 and DHPCW-02, and shear failure occurred in specimens DHPCW-03 and DHPCW-04. Figure 7 shows the failure mode and crack distribution in each specimen.
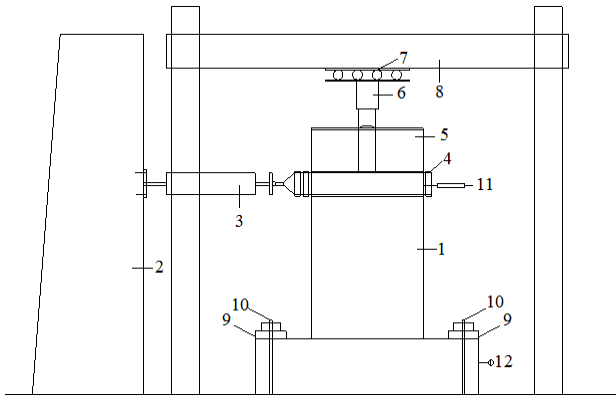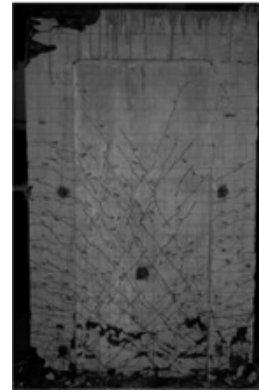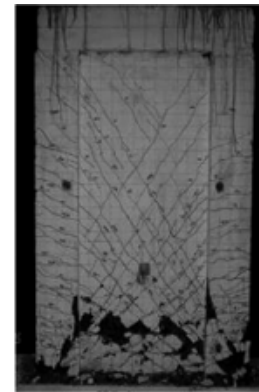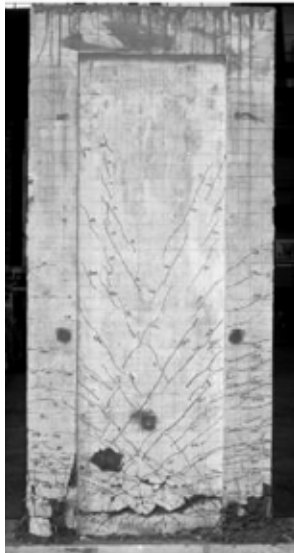
Figure 6. Test setup

Notes: 1.speciment 2.reaction wall 3.actuator 4. horizontal connection 5. Rigid beam 6.jack 7. sliding support 8.reaction frame 9.pressure beam 10.anchor bolt 11.displacement meter 12.dialgage
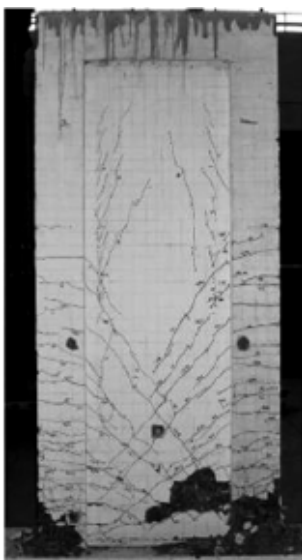

(a) DHPCW-01

(b) DHPCW-02

(c) DHPCW-03

(d) DHPCW-04

Figure 7. The failure mode and crack distribution in specimens

3.2 Comparison between Calculation and Experimental Results

According to the above calculation method, the boundary column and the wall web were divided into 1 and 5 fiber sections, respectively, while the wall was vertically divided into 4 units. According to *Code for design of concrete structures* [7], the conversion relationship between the cube compressive strength f_{cu} and the axial compressive strength f_c is given as follows:

$$f_c = 0.88\alpha_{c1}\alpha_{c2}f_{cu} \tag{1}$$

where α_{c1} is the ratio of prism strength and cube strength and α_{c2} is the brittleness reduction factor, which was assumed to be 0.82 and 0.87, respectively, for the C80 concrete. The axial compressive strength of the concrete in each specimen can be obtained according to Equation 1.

The parameters obtained from the concrete compression constitutive curve are as follows: $\sigma_U = f_c$, $\varepsilon_U = 0.0016$, $\varepsilon_L = 0.0021$, $\varepsilon_R = 0.0045$, $\varepsilon_X = 0.01$, $\sigma_Y = 39.8$MPa, and $\sigma_R/\sigma_U = 0.2$. The elastic modulus of C80 concrete is 38000 MPa [7]. The ε_X value of the reinforcement is 0.1. The elas-

tic modulus of reinforcement is determined according to *Code for design of concrete structures* [7].

Push-over analysis was carried out on all specimens. Figure 8 illustrates a comparison between the analysis and the test values of each specimen. Figure 8 shows that the analysis curve was in good agreement with the test curve. In addition, the initial stiffness, yield load, peak load, and ultimate displacement of the specimen were accurately simulated. The results verified the feasibility and accuracy of the elasto-plastic analysis method for high-strength concrete shear wall with boundary column using the fiber model
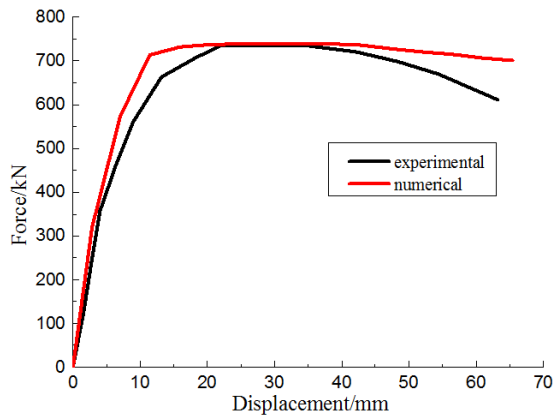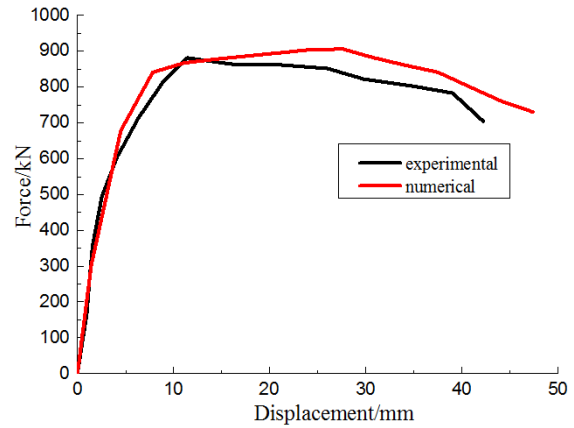

(a) DHPCW-01
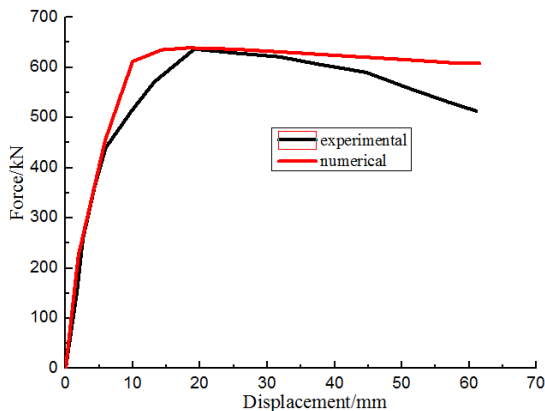
(b) DHPCW-02
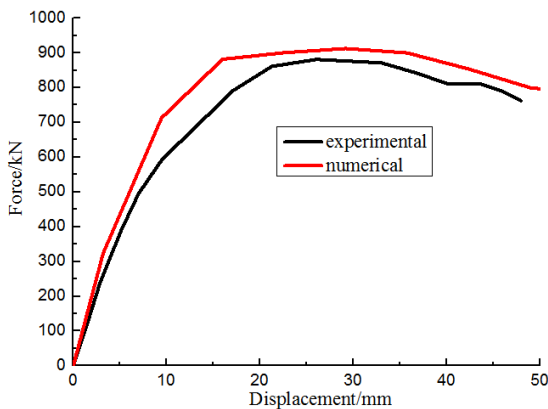
(c) DHPCW-03

(d) DHPCW-04

Figure 8. Comparison between the experimental and analysis results using skeleton curves

3.3 Parameter Analysis

In order to further study the seismic performance of high-strength concrete shear walls with boundary columns, the axial compression ratio, height to width ratio, ratio of vertical reinforcement, and ratio of longitudinal reinforcement in the boundary columns were selected for push-over analysis of high-strength concrete shear walls with boundary columns. The values of the parameters that were not set as variables in the analysis were set as the values obtained from DHPCW-02.

(1) Axial compression ratio

Figure 9 and Table 3 show the analysis results at different axial compression ratios (from 0.1 to 0.6). The yield displacement was calculated using the equal energy method [9]. The ultimate displacement was found to be the displacement corresponding to the peak load when it drops to 85% [10]. With the increase in the axial compression ratio, the bearing capacity first increased and then decreased, and the ultimate displacement showed a decreasing trend. At an axial compression ratio of 0.5, the bearing capacity reached 943.40 kN, which is 85.9 % higher than that obtained at an axial compression ratio of 0.1. However, the displacement ductility coefficient decreased from 6.45 to 4.99. At an axial compression ratio of 0.6, the bearing capacity slightly decreased at an axial compression ratio of 0.5. In addition, the ultimate displacement decreased to 16.62 mm, and the displacement ductility coefficient dropped to 1.82. Therefore, in order to ensure the seismic ductility of the shear wall with boundary columns, it was suggested that the axial compression ratio should not exceed 0.5.
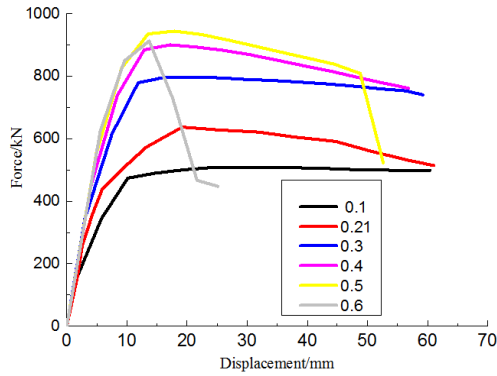
Figure 9. The effect of axial pressure ratio on the skeleton curve

Table 3. Test results under various axial compression ratios

axial compression ratio	bearing capacity	yield displacement	ultimate displacement	displacement ductility factor
0.1	507.37	9.36	60.42	6.45
0.21	648.92	9.69	61.06	6.30
0.3	796.88	9.54	59.21	6.21
0.4	899.42	9.95	56.12	5.64
0.5	943.40	9.80	48.91	4.99
0.6	912.51	9.13	16.62	1.82

(2) Height to width ratio

Figure 10 and Table 4 show the calculation results when the height to width ratio increased from 1.0 to 3.0. The increase in the height to width ratio causes the bearing capacity to decrease from 1291.21 kN to 485.07 kN, i.e., a 62.4% decrease. However, the ultimate displacement increased from 17.33 mm to 88.5 mm, and the ductility of displacement also gradually increased. The ductility coefficient of displacement increased from 3.85 to 6.67, i.e., it increased 1.73 times. These results show that the high-strength concrete shear wall with boundary columns exhibited good ductility with both low shear walls with a height to width ratio of 1.0 and high shear walls with a height to width ratio of 3.0.
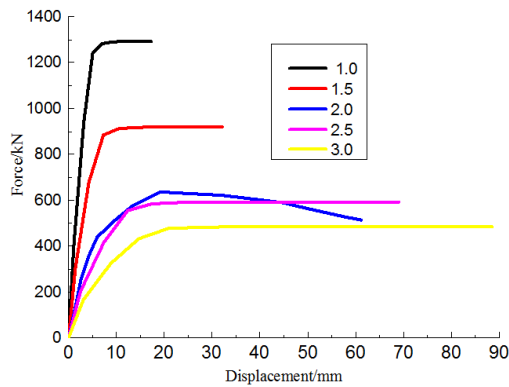

Figure 10. The influence of height to width ratio on skeleton curve

Table 4. The result for various height to width ratios

height to width ratio	bearing capacity	yield displacement	ultimate displacement	displacement ductility factor
1.0	1291.21	4.49	17.33	3.85
1.5	917.84	6.04	32.04	5.30
2.0	648.92	9.69	61.06	6.30
2.5	592.84	11.09	68.99	6.22
3.0	485.07	13.27	88.50	6.67

(3) Ratio of vertical reinforcement

Figure 11 and Table 5 show the effect of the ratio of vertical reinforcement on the high-strength concrete shear wall with boundary columns. When the ratio of vertical reinforcement increased from 0.55% to 1.31%, the bearing capacity increased only by 8.5%, and the ultimate displacement and displacement ductility coefficients remained almost unchanged. Therefore, the high-strength concrete shear wall with boundary columns do not require large number of vertically distributed rebars.
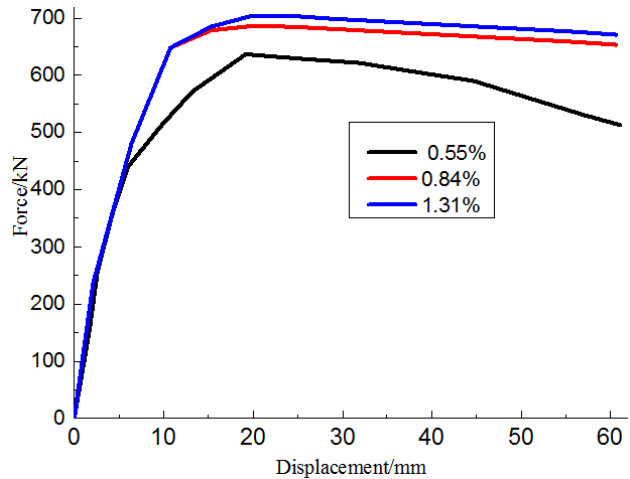

Figure 11. The effect of the vertical reinforcement ratio on skeleton curve

Table 5. The results of various ratios of vertically distributed reinforcements

ratio of vertical reinforcement	bearing capacity	yield displacement	ultimate displacement	displacement ductility factor
0.55%	648.92	9.69	61.06	6.30
0.84%	686.07	9.52	60.70	6.37
1.31%	704.07	10.09	60.65	6.02

(4) The ratio of longitudinal reinforcement in boundary columns

Figure 12 and Table 6 show the calculation results when the ratio of longitudinal reinforcement in boundary columns increased from 1.16% to 4.62%. This increase was accompanied with an increase in the bearing capacity from 507.23 kN to 711.45 kN, i.e., a 40.3% increase. The limit displacement slowly increased, while the ductility coefficient of displacement decreased at first and then slowly increased, because the yield displacement increased at first and then decreased. The displacement ductility coefficients were all greater than 6. Therefore, the ratio of longitudinal reinforcement in boundary columns had a significant impact on the bearing capacity, and increasing it could improve the bearing capacity of high-strength concrete shear wall with boundary columns.
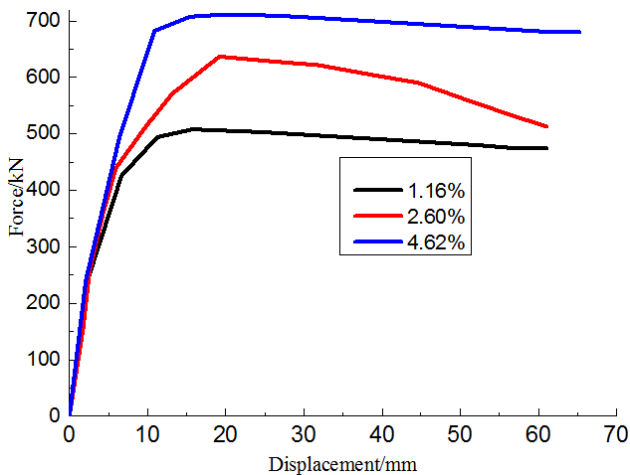

Figure 12. The effect of the ratio of longitudinal reinforcement in boundary columns on the skeleton curve

Table 6. Test results for various ratios of longitudinal reinforcement in the boundary columns

ratio of longitudinal reinforcement	bearing capacity	yield displacement	ultimate displacement	displacement ductility factor
1.16%	507.23	7.46	61.03	8.17
2.60%	648.92	9.69	61.06	6.30
4.62%	711.45	9.46	65.21	6.89

4. Conclusions

(1) The analysis results of the load-displacement curve were found to be close to the experimental results. The initial stiffness, yield load, peak load, and ultimate displacement of the specimen were found to be accurately simulated. Thus, the analysis method proposed here is able to accurately predict the bearing capacity, displacement, and ductility of high-strength concrete shear wall with boundary columns.

(2) The axial compression ratio was found to have a great impact on the bearing capacity and ductility of high-strength concrete shear walls with boundary columns. When the axial compression ratio increased from 0.1 to 0.6, the bearing capacity first increased and then decreased, and the ratio reached 0.6, the bearing capacity began to decrease. However, the ductility decreased in all cases, and the displacement ductility coefficient experienced a sudden change at an axial compression ratio of 0.6.

(3) As the height to width ratio increased from 1 to 3, the bearing capacity decreased by 62.4%, and the displacement ductility coefficient increased from 3.85 to 6.67, i.e., an increase of 1.73 times.

(4) The ratio of vertical reinforcement was found to have a little effect on the seismic behavior of high-strength concrete shear wall with boundary columns. Therefore, this type of walls should not be equipped with too many vertical rebars. The ratio of longitudinal reinforcement in boundary columns was found to have a significant effect on the bearing capacity, while the ductility was found to decrease at first and then slowly increase.

Acknowledgments

References

[1] Xingwen Liang, Penghui Yang, Xiaoling Cui, Mingke Deng, Xinghu Zhang. Experimental studies on seismic behavior of high strength concrete shear wall with boundary columns[J]. Journal of Building Structures, 2010, 31(1): 23-32.

[2] Fanglong He, Yapeng Zhu. A 3d model in nonlinear analysis of reinforced concrete shear wall with side column[J]. Engineering Mechanics, 2008, 25(6): 124-129.

[3] Graham H Powell. A state of the art educational event performance based design using nonlineal analysis[R]. Computers and Structures, Inc., 2007.

[4] Computers and Structures, Inc. Nonlinear anaysis and performance assessment for 3D structures user guide[M]. Berkeley, California, USA: Computers and Structures, Inc., 2006

[5] FEMA 356. Prestandard and commentary for the seismic rehabilitation of buildings[S]. Federal Emergency Management Agency:Washington, DC, 2000.

[6] Mander J B, Priestley M J N, Park R. Theoretical stress-strain model for confined concrete[J].Journal of structural engineering, 1988, 114(8): 1804-1826.

[7] GB 50010-2010 Code for design of concrete structures[S]. Beijing: China Communication Press, 2011: 63-64.

[8] Baolin Qin. Preliminary Evaluation on the Seismic Behavior of Super High-rise Structure Examples on the Support of PERFORM 3D Software[D].Chongqing: Chongqing University, 2012.

[9] Xiaolong Tong, Zhi Fang, Xiao Luo. Experimental study on seismic behavior of Reactive Powder Concrete shear walls[J]. Journal of Building Structures, 2016, 37(1): 21-30.

[10] Xiaowei Cheng, Xiaodong Ji, Richard S. Henry, Mengchao Xu. Coupled Axial Tension-Flexure Behavior of Slender Reinforced Concrete Walls[J]. Engineering Structures, 2019, 188: 261-276.